JOURNAL OF
THE ENGINEERING
MECHANICS DIVISION

Quadratic Limit States in Structural Reliability

By Bernd Fiessler,[1] Hans-Joachim Neumann,[2] and Rüdiger Rackwitz[3]

Introduction

In many engineering problems the quantification of the reliability of a structural facility subjected to random variability of its geometrical and material properties as well as uncertain loads or other actions upon it is required. Let reliability be measured in terms of a survival probability and each uncertain component be denoted as a basic uncertainty variable. Then, the computation of sensitive reliabilities for arbitrary structural problems in principle involves the evaluation of an n-dimensional volume integral. If, e.g., X is a vector of time and space independent basic variables with joint distribution function $F(\mathbf{x})$, then the probability of failure is one minus the reliability

$$P_f = 1 - \int_{(D)} df(\mathbf{x}) \quad \text{. . . . . (1)}$$

in which D = the domain in which the structure operates in safe states. The surface that separates the safe and unsafe domain is called failure surface or limit state function, which is taken to be associated with some given utility loss. For example, different failure surfaces would have to be formulated for structural collapse, yielding of a cross section, or exceedance of a given deformation limit at a certain point in the structure. Those failure surfaces must, at least implicitly, be expressed as functions of the basic uncertainty vector. And, of course, different target reliabilities would have to be set for each type of failure.

Note.—Discussion open until January 1, 1980. To extend the closing date one month, a written request must be filed with the Editor of Technical Publications, ASCE. This paper is part of the copyrighted Journal of the Engineering Mechanics Division, Proceedings of the American Society of Civil Engineers, Vol. 105, No. EM4, August, 1979. Manuscript was submitted for review for possible publication on May 25, 1978.

[1]Research Asst., Institut für Massivbau, Technical Univ. of Munich, Munich, W. Germany.
[2]Research Asst., Institut für Massivbau, Technical Univ. of Munich, Munich, W. Germany.
[3]Research Assoc., Institut für Massivbau, Technical Univ. of Munich, Munich, W. Germany.

Numerical integration over some arbitrary safe domain generally turns out to be rather tedious if feasible at all. Also, simulation methods are much too time-consuming to be applied generally so that simpler methods have been developed.

This paper first reviews the state of development of some methods that avoid explicit integration and examines their short-comings. In particular, the so-called "first-order reliability method" is studied. This method is, for the moment, based on a linearization of the functional relationship describing the failure surface. The method has been applied successfully to a number of engineering problems. Despite its conceptual simplicity, practical examples usually require the use of computers due to the complexity of the mechanical problem to be dealt with.

Doubts have been raised as to the accuracy of its probability estimates mainly because a linear approximation of the true failure surface appeared to be rather crude. Only in a few cases have results been checked by numerical integration displaying inaccurate results for some exceptional design situations. Therefore, the main body of this paper is dedicated to a more accurate method that may also be used to examine the accuracy of "first-order reliability methods."

Critical Review of Present First-Order Reliability Approaches

An effective alternative method to numerical integration has been proposed by Hasofer and Lind (1) and others. In its original form it reports reliability in terms of the safety index, β, and makes use only of the first and second statistical moments of the uncertainty vector. It is a discrete point checking method, measuring the minimum distance, β, between the boundary of the safe domain and the mean of the uncertainty vector in terms of standard deviations of the function describing the limit state. Consequently, not more than Tcheby-chev-type probability bounds can be derived which are not very useful in practice.

Even if the vector of uncertain variables, **X**, is an independent unit normal vector obtained from a general first and second moment description by suitable transformations, the safety index does not take proper account of the particular shape of the safe domain (see Ref. 6 or Ref. 12). In this case, the relationship

$$P\,[\text{Failure}] = P_f \geqq 1 - \phi\,(\beta) \quad (2)$$

is normally used for the estimation of failure probabilities and is associated with the simple tangential linearization of the limit state surface at the checking point. The $\phi\,(\cdot)$ is the univariate standard normal integral. Thereby, the checking point is the point $\mathbf{x}^*$ on the limit state surface in the formulation $g(\mathbf{x}) = 0$ which is nearest to the coordinate origin. The inequality sign in Eq. 2 is valid for convex safe regions. Another equally elementary and fairly conservative upper bound has been given as

$$P_f \leq 1 - \chi_n^2\,(\beta^2) \quad (3)$$

in which $\chi_n^2\,(\cdot)$ = the chi-squared distribution for n degrees-of-freedom (equals the dimension of the random vector **X**). This bound corresponds to a supporting hypersphere that substitutes the true failure surface. It is immediately recognized

that in this case P_f depends on n and, thus, the safety index, β, is no more dimension-invariant (see also Ref. 12). Depending on the values of n and β, both bounds are not always sufficiently close so that, in fact, the aforementioned objections apparently are justified, at least as long as the range of application of the simple reliability approach described before is not clearly defined. Several improvements to the method have recently been suggested by various authors.

One of these generalizations can deal with any distributional representation of the uncertainty vector in an approximate manner. Its particular form is now known as the "first-order reliability method" (9). In essence, it includes the transformation of non-normal basic uncertainty vectors into standard uncorrelated normal vectors and the linearization of the failure surface formulated in the new space at the point nearest to the coordinate origin yielding a parametric safety index, β. Various suitable algorithms have been proposed for the determination of that β (see, e.g., Refs. 1, 2, 7, and 9). Similarly, Eq. 2 is used to produce a first estimate of the failure probability. Numerical evaluation of Eq. 1 thus has been reduced to some transformation techniques and a problem of mathematical programming.

Further generalizations are made with respect to higher-order expansions of the limit state surface. Ditlevsen (1) developed sharper bounds for the true failure probability by calculating the probability content of inscribing and circumscribing rotational paraboloids. Those involve a convolution of a normal with a chi-square variable and will be explained in more detail in the sequel. Recently, the writers (7) investigated other approximating quadratic forms with rotational symmetry and gave suitable tables. The additional forms investigated are the hypersphere with the same (minimum or maximum) curvature in the checking point leading to the evaluation of the noncentral chi-square distribution and the rotational ellipsoid or hyperboloid both again involving operations with noncentral chi-square variables. Simple numerical integration is likewise required in the latter cases. Horne and Price (3) investigated the error in the failure probability given in Eq. 2 by studying an approximating hypersphere with radius corresponding to the mean curvature in the checking point.

If the safe domain is of a certain well-behaved shape, at least in the neighborhood of the checking point, these rotational forms clearly yield sharper bounds for the true failure probability. By taking the mean curvature one also arrives at better estimates for the failure probability than those obtainable by use of Eqs. 2 or 3. However, the limit state surface now must be continuous and twice differentiable since the second derivatives are used as additional information about the limit state surface. This is a more or less severe complication of such approaches. Also, physical reasoning must be used to choose among the parabolic, elliptical, or hyperbolic form.

The arbitrariness of the choice of suitable forms can be removed. In the following it is shown that there exist exact nonrotational quadrics whose probability content can be evaluated without undue difficulties. For convenience, we denote the methods involving second-order derivatives by "second-order reliability methods," in contrast to their "first-order" version, as outlined previously, and exact reliability methods.

The results on quadratic forms in normal variables given herein are not novel from a statistician's point of view but appear to be applied here for the first time in more detail to engineering problems.

General Derivation for Quadratic Forms

Assume that a given limit state surface is twice differentiable in the neighborhood of the checking point, P*, in the standardized and normalized coordinate system (X) of basic uncertain variables. Also, let the vector, X, be an independent vector.

The standardization requires the operation $X_i := (X_i - E[X_i])/D[X_i]$, whereas normalization is achieved by the transformation $X_i := \phi^{-1}[F(X_i)]$ for all components of X with $E[X_i]$ the mean, $D[X_i]$ the standard deviation, and $F(X_i)$ the distribution function of X_i. The direction cosines of the location vector of P* are given by the vector $\boldsymbol{\alpha}$ (see Fig. 1). Expand the limit state

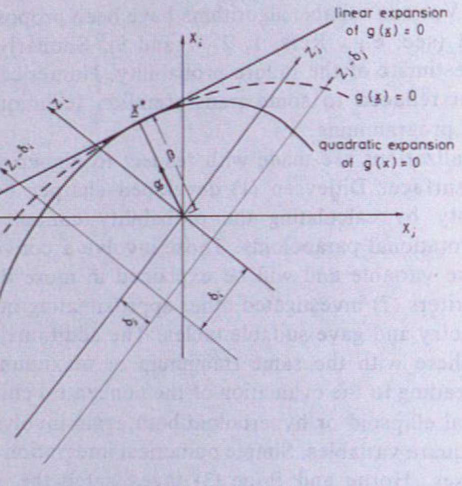

FIG. 1.—Linear and Quadratic Approximations to Limit State Surface $g(\mathbf{x}) = 0$

surface $g(\mathbf{x}) = 0$ into a second-order Taylor series about P*. Thus

$$g(\mathbf{x}) \equiv g(\mathbf{x}^*) + \frac{1}{1!}\sum_{i=1}^{n} \frac{\partial g(x)}{\partial x_i}\bigg|_{\mathbf{x}^*}(x_i - x_i^*) + \frac{1}{2!}\left[\sum_{i=1}^{n} \frac{\partial^2 g(x)}{\partial x_i^2}\bigg|_{\mathbf{x}^*}(x_i - x_i^*)^2 + 2\sum_{i=1}^{n-1}\sum_{j=i+1}^{n} \frac{\partial^2 g(x)}{\partial x_i \partial x_j}\bigg|_{\mathbf{x}^*}(x_i - x_i^*)(x_j - x_j^*)\right] = 0 \quad (4)$$

or in matrix notation, after some rearrangements, gives:

$$g(\mathbf{x}) = (\mathbf{x} - \mathbf{x}^*)^T \cdot \mathbf{G}_x \cdot (\mathbf{x} - \mathbf{x}^*) + 2 \cdot \mathbf{g}_x^T \cdot (\mathbf{x} - \mathbf{x}^*) + 2 \cdot g(\mathbf{x}^*) = 0 \quad (5)$$

in which $\mathbf{G}_x$ = the matrix of second and mixed derivatives; and $\mathbf{g}_x$ = the vector of first-order derivatives.

Eq. 5 constitutes a general quadric that can be brought into one of the standard forms in a new coordinate system (Z) by certain linear transformations (see Appendix I). If the $n - m$ variables occurring only in linear terms are denoted by $\bar{Z}$, it is

$$\sum_{i=1}^{n} \lambda_i (z_i - \delta_i)^2 = K_1 \quad (6)$$

$$\text{or} \quad \sum_{i=1}^{m} \lambda_i (z_i - \delta_i)^2 + \sum_{i=m+1}^{n} k_i \bar{z}_i = K_2 \quad (7)$$

in which λ_i are the eigenvalues of the matrix, G, and δ_i terms are the noncentralities in the Z coordinate system, whereas the constants K_1, K_2, and k_i, respectively, are determined by the transformation conditions (see Appendix I). If all $\lambda_i/K_{1,2}$ are greater than zero, the quadric is denoted by a positive definite. The positive definite case of Eq. 6 clearly is an ellipsoid with origin at the point $(\delta_1, \delta_2, ..., \delta_n)$ and semi-axis $[(K_1/\lambda_1)^{1/2}, (K_1/\lambda_2)^{1/2}, ..., (K_1/\lambda_n)^{1/2}]$. If some of the λ values are zero, cylindrical forms are obtained. The indefinite case is for λ with different signs. Further detailed classifications are given in Appendix I.

Since the Z variables are standardized uncorrelated normal variables, new stochastic variables, W and V, can be defined by

$$W = \sum_{i=1}^{n} \lambda_i (Z_i - \delta_i)^2 \quad (8)$$

$$V = \sum_{i=1}^{m} \lambda_i (Z_i - \delta_i)^2 + \sum_{i=m+1}^{n} k_i \bar{Z}_i \quad (9)$$

Obviously, the variable, W, is a linear combination of noncentral chi-squared distributed variables while the variable, V, additionally contains a linear combination of normally distributed variables. Therefore, the distribution function of W is simply the probability content of a spherical normal distribution over a region defined by Eq. 6. A similar interpretation holds for the variable, V. It follows from the definition of the safe domain in either of the forms $g(\mathbf{x}) > 0$ or $g(\mathbf{z}) > 0$ that the probability of failure is estimated by

$$P_f = P(W > K_1) = 1 - F_W(K_1) \quad (10)$$

$$P_f = P(V > K_2) = 1 - F_V(K_2) \quad (11)$$

Thus, the probability distribution functions of W and V must be known.

Distribution of W and V

Quadratic forms have received much less attention by statisticans than other problems involving normal variables. The statistical literature on this topic is exhaustively reviewed by Johnson/Kotz (5). However, only a few of the results available are useful in the context of structural reliability. They require the use of a computer, which in the light of its necessity in nontrivial engineering applications, anyhow, appears to be no serious obstacle.

In analogy to the noncentral chi-square distribution that can be expressed as mixtures of central chi-square distribution with weights given by the Poisson density, Ruben (10,11) showed that in the positive definite case the distribution of W can be given as an infinite mixture of chi-square probability functions.

Indefinite Case for W

Another quite general and useful expression for the indefinite case as well has been derived by Imhof (4). Imhof's solution is based on an inversion of the characteristic function of W. It is shown in Ref. 4 that the distribution function of W can be determined from

$$P(W > x) = \frac{1}{2} + \frac{1}{\pi}\int_0^{\infty} \frac{\sin\theta(u)}{u\,\rho(u)}\,du \quad (12)$$

with $$\theta(u) = \frac{1}{2}\sum_{j=1}^{n}[\tan^{-1}(\lambda_j u) + \delta_j^2 \lambda_j u (1 + \lambda_j^2 u^2)^{-1}] - \frac{1}{2} x u \quad (13)$$

$$\rho(u) = \prod_{j=1}^{n}(1 + \lambda_j^2 u^2)^{1/4} \exp\left\{\frac{\frac{1}{2}\sum_{j=1}^{n}(\delta_j \lambda_j u)^2}{1 + \lambda_j^2 u^2}\right\} \quad (14)$$

Eq. 12 must be evaluated by numerical quadrature. Finally, it is mentioned that for small failure probabilities the formulas given by Press (8) may be preferred.

General Parabolic Case

From Eqs. 9 or 11 it is seen that the variable, V, is the sum of a normal variable, Z_n, and a variable distributed like W but with fewer degrees-of-freedom, say m. Therefore, to obtain the distribution of V it is necessary to convolute a W variable with Z_n. It is

$$F(v) = \int_{-\infty}^{+\infty} \phi(z_n)\,F_W(v - z_n)\,dz_n \quad (15)$$

in which $\phi(\cdot)$ = the standard normal density; and $F_W(\cdot)$ = the distribution according to the foregoing two sections. Eq. 15 generally must be evaluated by an appropriate method of numerical integration.

Special Forms with Predetermined Principal Axis—General

It is possible to use other quadratic approximations to the boundary of the safe domain, $g(x) \equiv 0$, whose probability content can be calculated much easier in some cases and, therefore, shall be studied in some detail. In essence, such forms are set by preselecting the direction of their principal axis. Their curvatures in a nodal point are chosen as such to comply with the curvatures of the original limit state surface. But it should be clear that such forms may give an increasingly worse approximation to the true failure surface as the distance from the nodal point increases.

For example, let the original coordinate system (X) be rotated into a new system (Y) with the same origin such that the point P* is on the Y_n-axis and has coordinates (0, 0, ..., β) (see Fig. 2). Then, calculate the second-order and mixed derivatives in P* and rotate the system (Y) about the Y_n-axis such that the mixed derivatives vanish (see also Ref. 1). The new system has coordinates $z_1, z_2, \ldots, z_n = y_n$. Consequently, an approximating quadric derived from the

remaining diagonal $(n - 1)$ matrix of second-order derivatives has the same principal curvatures in the point P* (for further details see Appendix II). Then, either of the forms

$$\sum_{i=1}^{n-1} p_i z_i^2 + p_n(z_n - \delta_n)^2 = 1 \quad (16)$$

or $$\sum_{i=1}^{n-1} p_i z_i^2 - (z_n - \delta_n) = 0 \quad (17)$$

can be set with the coefficients p_i simply related to the curvatures in point P* (see Appendix II). Analogically to the section for general quadratic forms the left-hand part of Eqs. 16 and 17 represents a function of central or noncentral, linear or squared standard normal variables. Since Eqs. 16 and 17 are possible approximations to the true failure surface, the probability of failure is the

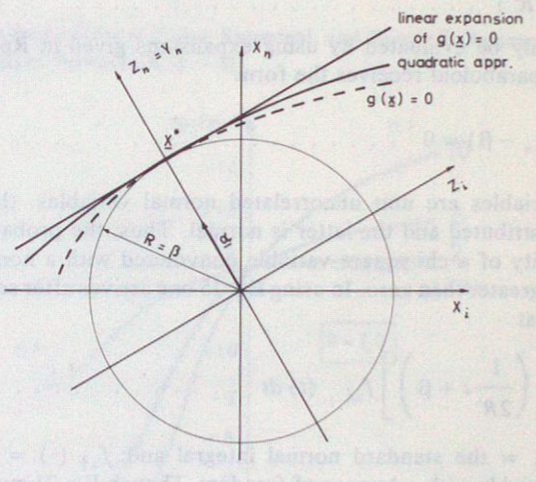

FIG. 2.—Derivation of Rotational Quadratic Forms

probability of a unit uncorrelated normal vector falling outside the domains defined by Eqs. 16 or 17. Thus, the formulas of the preceding sections likewise may be used to estimate the failure probability. It is noted that they simplify to a certain extent since only the noncentrality parameter, δ_n, is retained. As mentioned before, the choice of either a complete quadratic form or a paraboloid is now somewhat arbitrary. Information on the connectiveness of the safe domain and its convexity properties may be used to select the appropriate one.

Hyperspheres and Rotational Paraboloids

Major computational benefits are obtained when the forms, Eq. 16 or Eq. 17, are simplified towards rotational surfaces with the rotation axis being the Z_n-axis. The nodal curvature may be chosen as the mean of the principal curvatures, and so probability calculations may produce reliable estimates for the failure probability, or as the extreme curvatures to yield inscribing or circumscribing surfaces that result in upper and lower bounds for the failure probability.

Although rotational ellipsoids or two-shelled hyperboloids can principally be handled with the material presented herein, most gain is achieved if one concentrates on two elementary forms, i.e., the hypersphere and the rotational paraboloid, respectively. The former is obtained by taking the mean, maximum, or minimum curvature so that the quadric, Eq. 16, becomes

$$\sum_{i=1}^{n-1} z_i^2 + [z_n - (R+\beta)]^2 = R^2 \quad \ldots \ldots \ldots \ldots \ldots \ldots \ldots \ldots \ldots \ldots \ldots \ldots \ldots \ldots \ldots \ldots \ldots \ldots \ldots \ldots \ldots (18)$$

which is a hypersphere with radius R and center at the point (0, 0, ..., 0, $R + \beta$). If the Z variables are unit uncorrelated normal variables, the left-hand expression of Eq. 18 is known to be noncentral chi-square distributed with noncentrality parameter $\delta = [R + \beta]^2$ and, thus

$$P_f = 1 - \chi^2_{n,\delta}(R^2) \quad \ldots \ldots \ldots \ldots \ldots \ldots \ldots \ldots \ldots \ldots \ldots \ldots \ldots \ldots \ldots \ldots \ldots \ldots \ldots \ldots \ldots (19)$$

which can easily be evaluated by using expansions given in Ref. 5. Similarly, the rotational paraboloid receives the form

$$\frac{1}{2R}\sum_{i=1}^{n-1} z_i^2 - (z_n - \beta) = 0 \quad \ldots \ldots \ldots \ldots \ldots \ldots \ldots \ldots \ldots \ldots \ldots \ldots \ldots \ldots \ldots \ldots \ldots \ldots \ldots \ldots \ldots (20)$$

If the Z variables are unit uncorrelated normal variables, the first term is chi-squared distributed and the latter is normal. Thus, the probability of failure is the probability of a chi-square variable convoluted with a noncentral normal variable being greater than zero. In using Eq. 15 one arrives after some elementary manipulations at

$$P_f = \int_0^\infty \phi\left[-\left(\frac{1}{2R}t + \beta\right)\right] f_{\chi^2_{n-1}}(t)\,dt \quad \ldots \ldots \ldots \ldots \ldots \ldots \ldots \ldots \ldots \ldots \ldots \ldots \ldots \ldots \ldots \ldots \ldots \ldots \ldots \ldots \ldots (21)$$

in which $\phi[\cdot]$ = the standard normal integral and; $f_{\chi^2_\nu}(\cdot)$ = the density of a chi-square variable with ν degrees-of-freedom. Though Eq. 21 must be evaluated by numerical quadrature, accurate results generally can be obtained easily. Also, some tables are available in Refs. 1 and 7.

Review and Examples

A general view of the dependence of P_f on the safety index, β, the curvature in the checking point, and the dimension of the basic variable vector can be gained when considering simple examples of rotational symmetry. In Fig. 3 a two-dimensional case is demonstrated for $\beta = 3$ showing the plane, spherical, and parabolic approximations for various curvatures in the checking point. It shows the relation between probability of failure calculated for hyperplanes, rotational hyperparaboloids, and hyperspheres versus the dimension of the uncertainty vector, X. Additionally, Fig. 4 expresses the sensitivity of the failure probability versus the dimension of X and the curvature in the checking point for two reliability levels as expressed by $\beta = 3$ and $\beta = 7$. It can be seen that the differences between linear and quadratic approximations of the failure

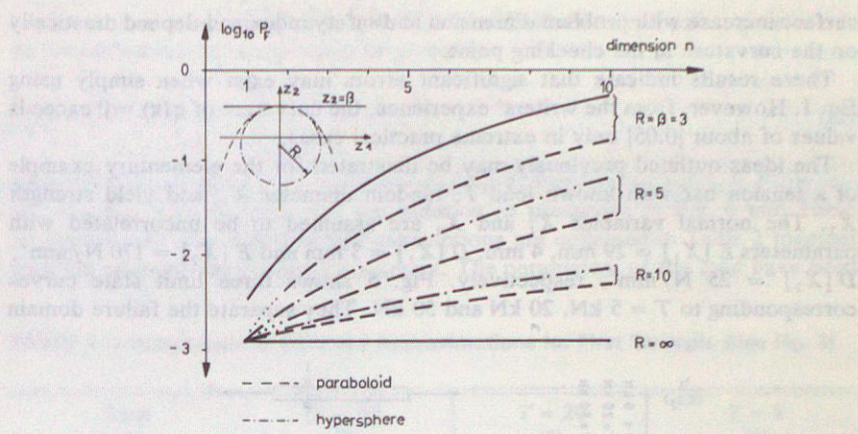

FIG. 3.—Failure Probability of Plane, Spherical, and Parabolic Approximations of $g(x) = 0$ versus Problem Dimension ($\beta = 3$)

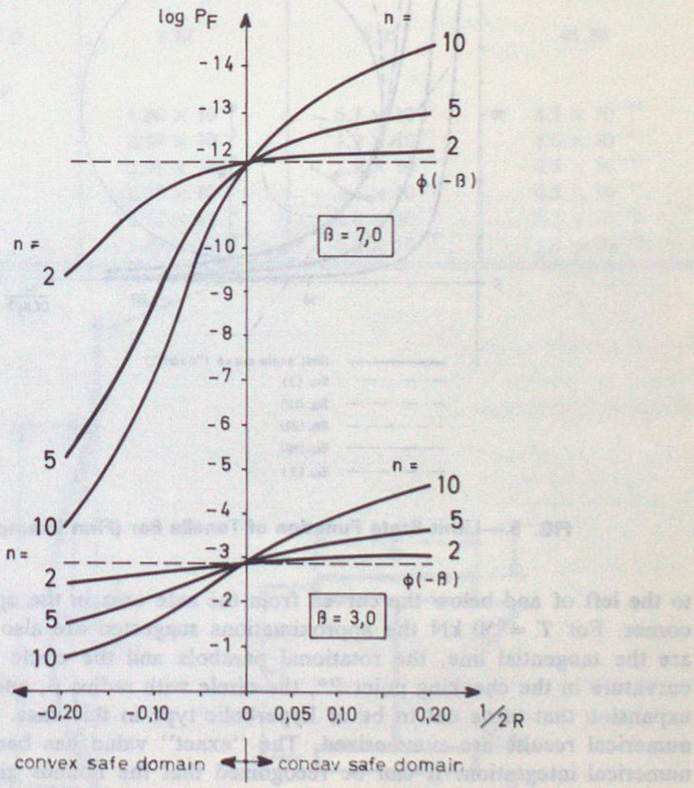

FIG. 4.—Failure Probability of Paraboloids for $\beta = 3$ and $\beta = 7$ versus Problem Dimension

surface increase with problem dimension and safety index and depend drastically on the curvature in the checking point.

These results indicate that significant errors may exist when simply using Eq. 1. However, from the writers' experience, the curvature of $g(x) = 0$ exceeds values of about $|0.05|$ only in extreme practical cases.

The ideas outlined previously may be illustrated for the elementary example of a tension bar with known load T, random diameter X_1, and yield strength X_2. The normal variables X_1 and X_2 are assumed to be uncorrelated with parameters $E[X_1] = 29$ mm, 4 mm, $D[X_1] = 3$ mm and $E[X_2] = 170$ N/mm^2, $D[X_2] = 25$ N/mm^2, respectively. Fig. 5 shows three limit state curves corresponding to $T = 5$ kN, 20 kN and 50 kN. They separate the failure domain

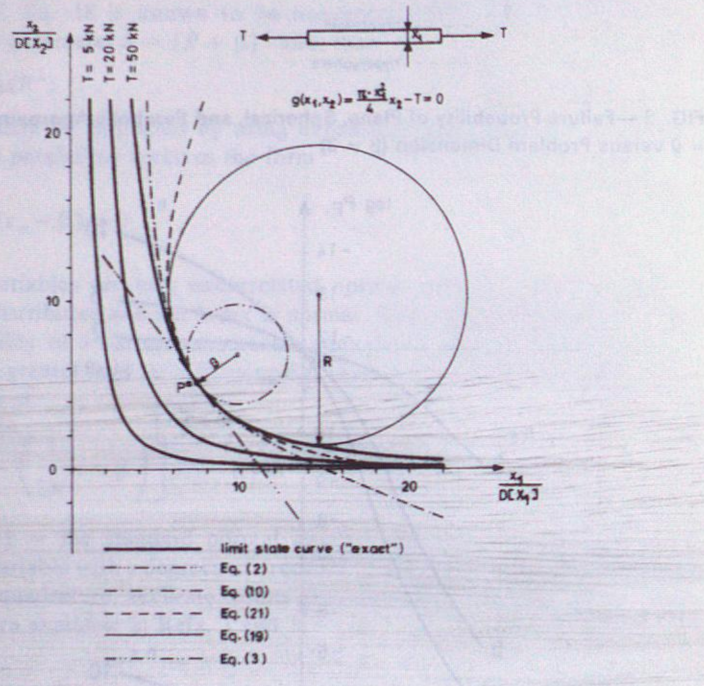

FIG. 5.—Limit State Function of Tensile Bar (First Example)

to the left of and below the curves from the safe area in the upper right-hand corner. For $T = 50$ kN the approximations suggested are also drawn. These are the tangential line, the rotational parabola and the circle with the same curvature in the checking point P*, the circle with radius β, and the quadratic expansion that turns out to be of hyperbolic type in this case. In Table 1 the numerical results are summarized. The "exact" value has been obtained by numerical integration. It can be recognized that the bounds given by Eqs. 2 and 3 include all results. In each case the various quadratic approximations are quite close to the exact result. With the exception of the bound according to Eq. 3 the differences are negligible from an engineering point of view.

As a second example an eccentrically loaded T-shaped steel column is studied. Its simplified failure surface can be given by

$$g(\mathrm{x}) \equiv x_1 - x_2\left(\frac{1}{A} + \frac{f}{W}\right) = 0 \quad (22)$$

with $A = (x_4 + x_5)\,x_6$; $W = (x_4 + x_5)\,x_3$; $f = x_7/(1 - x_2/P_E)$; $P_E = x_8\,(x_4 + x_5)\,(x_3/2)^2\,(\pi/L)^2$; and the notation as presented in Fig. 6 and Table 2, respectively. The distributional assumptions are collected in Table 2 together with the selected distribution parameters. The parameters of the load have been

TABLE 1.—Comparison of Different Approximations for First Example (See Fig. 5)

Case (1)	$T = 50$ (2)	$T = 20$ (3)	$T = 5$ (4)
Checking point P* $\{x_1^*, x_2^*\}$	22.4, 127.1	17.25, 85.53	28.05, 8.09
Safety index β	2.902	5.273	6.492
Radius of curvature R	8.81	6.05	45.30
Failure probability			
Eq. 2	1.86×10^{-3}	6.7×10^{-8}	4.3×10^{-11}
Eq. 12	2.29×10^{-3}	1.9×10^{-7}	5.0×10^{-11}
Eq. 19	2.31×10^{-3}	1.9×10^{-7}	4.5×10^{-11}
Eq. 21	2.29×10^{-3}	1.6×10^{-7}	4.5×10^{-11}
"Exact"	2.32×10^{-3}	2.0×10^{-7}	5.5×10^{-11}
Eq. 3	1.49×10^{-2}	9.2×10^{-7}	5.0×10^{-10}

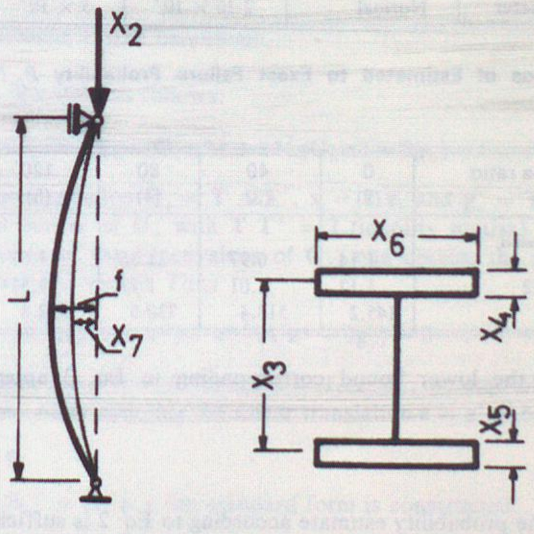

FIG. 6.—Notations for Second Example (Column Buckling)

chosen such that the same safety index of $\beta = 3.434$ is valid for each slenderness ratio. Note that in this case the standardization and normalization operations, as described in the sections just preceding Eq. 4, have to be applied by introducing further nonlinearities into the failure surface Eq. 22. Table 3 shows the ratio of estimated to "exact" failure probabilities, the latter being computed by Monte Carlo simulation. In varying the slenderness ratio of the column this example covers a wide range of possibilities with respect to signs and values of curvatures. The results obtained either by linear or quadratic approximations are fairly good whereas the lower bound corresponding to Eq. 3 appears to be too conservative.

TABLE 2.—Distribution and Parameter Assumptions for Second Example (see Fig. 6)

Type of variable (1)	Distribution type (2)	Mean (3)	Standard deviation (4)	Coefficient of variation (5)
Yield strength, x_1, in Newtons per square millimeter	Log-normal	320	30	0.094
Load, x_2, in Newtons	Gumbel	variable	—	0.150
Column depth, x_3, in millimeters	Normal	160	1.5	0.009
Flange width, x_4, x_5, in millimeters	Log-normal	7.8	0.4	0.051
Column breadth, x_6, in millimeters	Normal	82	0.8	0.010
Eccentricity, x_7, in millimeters	Normal	0	$L/1770$	—
Young's modulus, x_8, in Newtons per square millimeter	Normal	2.16×10^5	5×10^3	0.023

TABLE 3.—Ratios of Estimated to Exact Failure Probability $P_{f,i}/P_{f,\text{exact}}$ (Second Example)

Slenderness ratio (1)	0 (2)	40 (3)	80 (4)	120 (5)	160 (6)
$P_{f,i}/P_{f,\text{exact}}$					
Eq. 2	1.14	0.97	1.36	1.67	2.50
Eq. 12	1.12	1.01	1.17	1.51	1.18
Eq. 3	145.2	518.4	730.5	892.8	1,339

Conclusions

In general, the probability estimate according to Eq. 2 is sufficiently accurate. This conclusion holds for the majority of complex engineering problems in higher

dimensions as long as the reliability level is not too high and the uncertainty vector has distributions not too far from the normal. If the original uncertainty vector has a distribution function that deviates significantly from the normal, originally sufficiently smooth failure surfaces can become distinctively curved in the normalized space. The curvature caused by the necessary probability distribution transformation may actually overrule by far those given by the mechanical problem and their effect increases with problem dimension. Only then may the simple estimates following Eq. 2 be less adequate. The first and third writers (9) have shown that adopting the foregoing "second-order" approach in the space of normalized variables will yield accurate probability estimates even in those cases. The use of quadratic forms appears even more appropriate in parametric cases, e.g., for time-dependent reliability problems. It should, however, be mentioned that the second-order reliability method as outlined previously still remains a single point checking method. Like its "first-order" version it fails to give accurate results as soon as the location of the checking point and the curvature of the failure surface in it is not sufficiently representative for the entire shape of the safe domain. Then, other methods are in order that obviously still have to be worked out, perhaps on the lines suggested in Ref. 12. With this restriction a simplified second-order reliability method, e.g., a method on the basis of the noncentral chi-square distribution, that only takes account of the mean curvature can be recommended to replace the simplier methods.

Acknowledgments

This study has partially been carried out while the third writer was on leave at the Danish Technical University and Danish Engineering Academy. The use of their facilities is appreciated. The writers gratefully acknowledge O. Ditlevsen's initiating comments on some of their earlier studies in first-order reliability.

Appendix I.—Quadratic Taylor Expansions

Eq. 5 can be rewritten as follows:

$$g(\mathbf{x}) = \mathbf{x}^T \cdot \mathbf{G}_x \mathbf{x} + 2\mathbf{x}^T(\mathbf{g}_x - \mathbf{G}_x \mathbf{x}^*) + \mathbf{x}^{*T}(\mathbf{G}_x \mathbf{x}^* - 2\mathbf{g}_x) = 0 \qquad (23)$$

In using the transformation $\mathbf{G}_x = \mathbf{T}\,\Lambda\,\mathbf{T}^T$, $\mathbf{x} = \mathbf{T}\,\mathbf{z}$, and $\mathbf{g}_x = \mathbf{T}\,\mathbf{g}_z$, in which $\mathbf{T}$ = the modal matrix of $\mathbf{G}_x$ with $\mathbf{T}\cdot\mathbf{T}^T = \mathbf{I}$ (identity matrix) and $\Lambda = (\lambda_i)$ the diagonal matrix of the Eigenvalues of $\mathbf{G}_x$, one obtains the principal form where all mixed terms vanish. Thus

$$g(\mathbf{z}) = \mathbf{z}^T \cdot \Lambda\,\mathbf{z} + 2\mathbf{z}^T(\mathbf{g}_z - \Lambda\cdot\mathbf{z}^*) + \mathbf{z}^{*T}(\Lambda\,\mathbf{z}^* - 2\mathbf{g}_z) = 0 \qquad (24)$$

If $\mathbf{G}_x$ is regular, i.e., $\lambda_i \neq 0$ for all $i = 1, 2, \ldots, n$, Eq. 24 represents a complete quadric. After applying the linear translation $\mathbf{z} = \mathbf{z}' + \delta$ which implies

$$\delta = \mathbf{z}^* - \Lambda^{-1} \cdot \mathbf{g}_z \qquad (25)$$

and, of course, $\Lambda^{-1} = (1/\lambda_i)$, the standard form is constructed:

$$(\mathbf{z} - \delta)^T \Lambda (\mathbf{z} - \delta) = \mathbf{g}_z^T \Lambda^{-1} \mathbf{g}_z \qquad (26)$$

or $$\sum_{i=1}^{n} \lambda_i (z_i - \delta_i)^2 = K_1 \qquad (27)$$

with $K_1 = \mathbf{g}_z^T \Lambda^{-1} \mathbf{g}_z$ and which is the same as Eq. 6.

If G_x is singular, i.e., some of the λ values equal zero [the case where all λ equals zero is of no further interest since $g(\mathbf{x}) = 0$ is linear in each component of X] and the corresponding elements of $\mathbf{g}_z$ vanish, too, then cylindrical forms are obtained. Such forms are dealt with as complete quadrics but with a smaller dimension.

One arrives at parabolic forms if for some components of **Z** it is $\lambda_i = 0$, but $g_{z,i} \neq 0$. In general, it is

$$(\mathbf{z} - \boldsymbol{\delta})^T \Lambda (\mathbf{z} - \boldsymbol{\delta}) + 2\bar{\mathbf{z}}^T \mathbf{g}_z = K_2 \qquad (28)$$

with K_2 similar to K_1 but without the terms where $\lambda_i = 0$ and $\bar{\mathbf{z}}$ = the vector of these components for which the foregoing conditions hold; and $\boldsymbol{\delta}$ contains only the nonzero components for which the conditions are not valid, specifically all components in which $\lambda_i \neq 0$. Finally, the standard form Eq. 28 can be written in the form of Eq. 7:

$$\sum_{i=1}^{m} \lambda_i (z_i - \delta_i)^2 + 2 \sum_{i=m+1}^{n} \bar{z}_i g_{z_i} = K_2 \qquad (29)$$

in which K_2 is given by the right-hand side of Eq. 28. For convenience, the components of **z** in Eq. 29 have been ordered to include the m quadratic terms in the first part and the $n - m$ linear terms in the second part of the left-hand side of Eq. 29.

Appendix II.—Principal Curvatures in Checking Point P*

Let the checking point P* with the vector of direction cosines $\boldsymbol{\alpha}$ be found by a suitable algorithm in the (X) space. There always exists an orthogonal rotation matrix, **T**, such that the Y_n-axis of the new coordinate system is parallel to the vector $\boldsymbol{\alpha}$. Thus

$$\mathbf{Y} = \mathbf{T}^T \cdot \mathbf{X} \qquad (30)$$

Clearly, the last column vector of **T** is the vector α. The other columns may be found by one of the well-known orthogonalization procedures. In the new system it is for the derivatives $g_{y,i} = \partial g(y)/\partial y\,|_{y^*}$. Thus

$$g_{y,i} = 0 \quad \text{for} \quad i = 1, 2, \ldots, n-1 \qquad (31)$$

The matrix, $\mathbf{G}_y$, of second and mixed derivatives in P* is a symmetrical matrix with the nth column and row deleted. In applying elementary results of differential geometry, e.g., the two Gaussian fundamental theorems for curves on n-dimensional surfaces, the principal curvatures in P* are obtained from the roots of the characteristic equation:

$$\det\left(\frac{1}{g_{y,n}} \mathbf{G}_y - \kappa \cdot \mathbf{I}\right) = 0 \qquad (32)$$

Then, the radius of curvature in P* with respect to the ith principal axis

is $R_i = 1/\kappa_i$. In order to establish suitable quadratic forms with the same principal curvatures we set

$$(\mathbf{z} - \boldsymbol{\delta})^T \mathbf{P} (\mathbf{z} - \boldsymbol{\delta}) = 1 \qquad (33)$$

in which $\boldsymbol{\delta} = (0, 0, \ldots, \delta_n)$; and P = the diagonal matrix of coefficients indicating the length of the semi-axis, a_i, by the relation, $p_i = 1/a_i^2$. The semi-axis, a_i, depends on the curvatures by $a_i^2 = a_n/\kappa_i$. The requirement that Eq. 34 has the same gradient in P* as the original form leads to $p_n = g_{y_n}^2/4$, whereas the other elements p_i can be calculated by using the aforementioned relationship between semi-axis and curvatures in the nodal point. It is immediately deducted that

$$p_i = -\frac{\kappa_i g_{x_n}}{2} \quad \text{for} \quad i = 1, 2, \ldots, n-1 \qquad (34)$$

Of course, the radius is given by $R_i = 1/\kappa_i$. With these expressions Eq. 16 can easily be derived. Similarly, the relations between nodal curvatures and coefficients p_i are used in the parabolic case. Here, it is

$$p_i = \frac{\kappa_i}{2} \qquad (35)$$

Thus, also Eq. 17 of the main text may be set with the p values as given by Eq. 35 and $\delta_n = \beta$.

For rotational forms the curvatures correspond to

$$\kappa = \frac{1}{m}\sum_{i=1}^{m} \kappa_i \quad \text{or} \quad \kappa = \min_{i=1}^{m} \{\kappa_i\} \quad \text{or} \quad \kappa = \max_{i=1}^{m} \{\kappa_i\} \qquad (36)$$

whatever type is selected, with m being the number of quadratic terms in Eqs. 16 or 17.

Appendix III.—References

1. Ditlevsen, O., "Evaluation of the Effect on Structural Reliability of Slight Deviations from Hyperplane Limit State Surfaces," *Proceedings,* Second International Workshop on Code Formats in Mexico City, *DIALOG 2-76,* Danmarks Ingeniørakademi, Lyngby, Denmark, Jan., 1976.
2. Hasofer, A. M., and Lind, N. C., Exact and Invariant Second-Order Code Format," *Journal of the Engineering Mechanics Division,* ASCE, Vol. 100, No. EM1, Proc. Paper 10376, Feb., 1974, pp. 111–121.
3. Horne, R., and Price, P. H., "Commentary on the Level-II-Procedure," *Rationalisation of Safety and Serviceability Factors in Structural Codes, CIRIA Report 63,* Construction Industry Research and Information Association, London, England, 1977.
4. Imhof, J. P., "Computing the Distribution of Quadratic Forms in Normal Variables," *Biometrika,* Vol. 48, Nos. 3 and 4, 1961, pp. 419–426.
5. Johnson, N. I., and Kotz, S., *Distributions in Statistics—Continuous Univariate Distributions—2,* Houghton Mifflin Co., Boston, Mass., 1970.
6. Lind, N. C., "Formulation of Probabilistic Design," *Journal of the Engineering Mechanics Division,* ASCE, Vol. 103, No. EM2, Proc. Paper 12861, Apr., 1977, pp. 273–284.
7. Neumann, H.-J., Fiessler, B., and Rackwitz, R., "Die genäherte Berechnung der Versagenswahrscheinlichkeit mit Hilfe rotationssymmetrischer Grenzzustandsflächen 2. Ordnung," *SFB 96,* Technical University of Munich, Ber. zur Sicherheitstheorie der Bauwerke, No. 22, 1977.

8. Press, S. J., "Linear Combinations of Non-Central χ^2-Variates," *Annals of Mathematical Statistics,* Vol. 37, 1966, pp. 480–487.
9. Rackwitz, R., and Fiessler, B., "Non-normal Distributions in Structural Reliability," *SFB 96,* Technical University of Munich, Ber. zur Sicherheitstheorie der Bauwerke, No. 29, 1978, pp. 1–22.
10. Ruben, H., "Probability Content of Regions under Spherical Normal Distributions, IV," *Annals of Mathematical Statistics,* Vol. 33, 1962, pp. 542–570.
11. Ruben, H., "A New Result of the Distribution of Quadratic Forms," *Annals of Mathematical Statistics,* Vol. 34, 1963, pp. 1582–1584.
12. Veneziano, D., "Contributions to Second Moment Reliability Theory," *Research Report R74-33,* Department of Civil Engineering, Massachusetts Institute of Technology, Cambridge, Mass., 1974.

Appendix IV.—Notation

The following symbols are used in this paper:

$\mathbf{A}, \mathbf{A}^T$ = matrix, transposed matrix;
$\mathbf{a}, \mathbf{a}^T$ = column vector, row vector;
$D(X)$ = standard deviation of X;
$E(X)$ = expectation (mean) of X;
$F(\cdot)$ = probability distribution function;
$f(\cdot)$ = probability density function;
$g(\mathbf{x})$ = state function of $\mathbf{x}$;
P = probability;
P_f = probability of failure;
X, Z = random variables;
$\mathbf{x}^*$ = location vector of checking point P*;
$\boldsymbol{\alpha}$ = vector of direction cosines of checking point P*;
β = reliability index;
$\Phi(\cdot)$ = standard normal probability function;
$\Phi^{-1}(\cdot)$ = inverse standard normal probability function;
$\phi(\cdot)$ = standard normal density function;
χ_n^2 = (central) chi-square distribution with n degrees-of-freedom; and
$\chi_{n;\delta}^2$ = noncentral chi-square distribution with n degrees-of-freedom and noncentrality parameter δ.

14739 QUADRATIC LIMIT STATES IN RELIABILITY

KEY WORDS: **Limit design method;** Probability; Quadratic forms; **Reliability; Structural stability**

ABSTRACT: Second-moment methods are widely applied in structural reliability. Recently, so-called first-order reliability methods have been developed that are capable of producing reliable estimates of the failure probability for arbitrary design situations and distributional assumptions for the uncertainity vector. In essence, nonlinear functional relationships or probability distribution transformations are approximated by linear Taylor expansions so that the simple second-moment calculus is retained. Failure probabilities are obtained by evaluating the standard normal integral, which is the probability content of a circular normal distribution in a domain bounded by a hyperplane. In this paper second-order expansions are studied to approximate the failure surface and some results of the statistical theory of quadratic forms in normal variates are used to calculate improved estimates of the failure probability.

REFERENCE: Fiessler, Bernd, Neumann, Hans-Joachim, and Rackwitz, Rudiger, "Quadratic Limit States in Structural Reliability," *Journal of the Engineering Mechanics Division*, ASCE, Vol. 105, No. EM4, **Proc. Paper 14739**, August, 1979, pp. 661-676